

The Fundamental Solution of the One-Dimensional Elliptic Operator and its Application to Solving the Advection-Diffusion Equation

Ronald Mwesigwa^{1*}, GodwinKakuba² and David Angwenyi³

¹Mbarara University of Science and Technology, Uganda

²Masinde Muliro University of Science and Technology, Kenya

Abstract

The advection-diffusion equation is first formulated as a boundary integral equation, suggesting the need for an appropriate fundamental solution to the elliptic operator. Once the fundamental solution is found, then a solution to the original equation can be obtained through convolution of the fundamental solution and the desired right hand side. In this work, the fundamental solution has been derived and tested on examples that have a known exact solution. The model problem here used is the advection-diffusion equation, and two examples have been given, where in each case the parameters are different. The general approach is that the time derivative has been approximated using a finite difference scheme, which in this case is a first order in Δt , though other schemes may be used. This may be considered as the time-discretization approach of the boundary element method. Again, where there is need for finding the domain integral, a numerical integration scheme has been applied. The discussion involves the change in the errors with an increase in Δx . Again, for small solution values, considering relative errors at selected points along the domain, and how they vary with different choices of Δx and Δt . The results indicate that at a given value of x , errors increase with increasing Δx , and again as $R\Delta$ increases, the magnitudes of the errors keep increasing. The stability was studied in terms of how errors from one time step do not lead to high growth of the errors in subsequent steps.

Keywords: Fundamental solution • Boundary element method • Advection-diffusion equation • Time-discretisation

Introduction

Fundamental solutions can be applied in finding the numerical solution of partial differential equations by the boundary element method. The term boundary element method (BEM) denotes any method for the approximate numerical solution of boundary integral equations, a classical tool for the analysis of boundary value problems for partial differential equations [1]. More broadly, BEM has been used as a generic term for a variety of numerical methods that use a boundary or boundary-like discretization [2]. These can include the general numerical implementation of boundary integral equations, known as the boundary integral equation method, whether elements are used in the discretization or not; or the method of fundamental solutions in which the fundamental solutions are distributed outside the domain in discrete or continuous fashion with or without integral equation formulation; among others. The different algorithms of BEM for parabolic equation are presented in [3], such as the time-discretization and the Laplace transform. The one-dimensional hyperbolic equation supplemented by adequate boundary and initial conditions is considered in [4]. This equation is solved using the combined variant of the BEM and in an analytical way. The dual phase lag equation describing the temperature field in a 3D domain is solved by means of the boundary element method using discretization in time, while at the same time the Dirichlet and Neumann boundary conditions are taken into account [5]. Numerical realization of the BEM for the constant boundary elements and constant internal cells is presented. With the increasing importance of numerical techniques for solving boundary value problems, integral equation methods are becoming

more and more popular as a starting point for numerically solving boundary value problems for the reasons listed in [6], one of which is, the arising large systems of linear equations are typically better conditioned as the direct finite element discretizations of the underlying boundary value problem. A numerical method based on the boundary integral equation and an application of the dual reciprocity BEM has been used to solve the second-order one space-dimensional hyperbolic telegraph equation. Also the time stepping scheme is employed to deal with the time derivative [7]. The application of the dual reciprocity method to the time-stepping BEM for the solution of the transient heat conduction problems in homogeneous as well as inhomogeneous materials has been presented in [8,9]. The integral equation formulation employs the fundamental solution of the Laplace equation for homogeneous materials, and hence domain integrals arise in the boundary integral equation. Furthermore, time derivative is approximated by the time-stepping method, and the domain integral also appears from this approximation. This article suggests how BEM using time-discretisation may be applied to solving the advection-diffusion equation, where the fundamental solution to the elliptic operator has played a major role. Advection-diffusion models are intended to make predictions through solution of the so-called advection-diffusion equation, which makes use of probability, time, velocity and the diffusion coefficient with spatial variability, and reflects two transport mechanisms: advective (or convective) transport with the mean flow, and diffusive transport due to concentrations gradients. The models are typically ran over a medium term period, say, days to months and they are generally limited to small spatial scales.

Problem Formulation

Consider the following one-dimensional advection-diffusion equation:

$$\frac{\partial u}{\partial t}(x, t) = D(x) \frac{\partial^2 u}{\partial x^2}(x, t) - c(x) \frac{\partial u}{\partial x}(x, t), \quad (1)$$

such that $x \in [a, b]$ and $t \in [0, T]$, with initial condition

$$u(x, 0) = u_0(x),$$

and boundary conditions $u(a, t) = g_0(t)$, $u(b, t) = g_1(t)$,

*Address for Correspondence: Ronald Mwesigwa, Mbarara University of Science and Technology, Uganda, E-mail: rsmwesigwa@gmail.com

Copyright: © 2020 Mwesigwa R, et al. This is an open-access article distributed under the terms of the Creative Commons Attribution License, which permits unrestricted use, distribution, and reproduction in any medium, provided the original author and source are credited.

Received 27 October 2020; Accepted 12 November 2020; Published 19 November 2020

where $c(x)$ and $D(x)$ are arbitrary functions, though the formulation here is based on c, D constant. Also, $D(x) \neq 0$, and it is assumed that $g_0(t)$ and $g_1(t)$ are smooth functions over the given interval.

Developing boundary integral equations

To solve (8), the BEM using discretization in time is applied. The time interval $[0, T]$ is divided into n pieces, each of length $\Delta t = T/n$. The corresponding points are denoted t_j , for $j = 0, 1, \dots, n$. The ends of the interval are $t_0 = 0$ and $t_n = T$; the interior points are $t_j = j\Delta t$ for $j = 1, 2, \dots, n - 1$. For the time interval $[t_j, t_{j+1}]$ the following approximation of time derivative can be used

$$\frac{\partial u}{\partial t}(x, t_j) = \frac{u(x, t_{j+1}) - u(x, t_j)}{\Delta t}$$

so that

$$D \frac{\partial^2 u}{\partial x^2}(x, t_{j+1}) - c \frac{\partial u}{\partial x}(x, t_{j+1}) - \frac{u(x, t_{j+1}) - u(x, t_j)}{\Delta t} = 0 \quad (2)$$

At the t -th time step, (8) can be approximately rewritten as

$$D \frac{\partial^2 u^{j+1}(x)}{\partial x^2} - c \frac{\partial u^{j+1}(x)}{\partial x} - \frac{1}{\Delta t} u^{j+1}(x) + \frac{1}{\Delta t} u^j(x) = 0$$

where $u(x) \equiv u(x, t)$. The weighted residual criterion is applied to (2) to obtain

$$\int_a^b \left(D \frac{\partial^2 u^{j+1}(x)}{\partial x^2} - c \frac{\partial u^{j+1}(x)}{\partial x} - \frac{1}{\Delta t} u^{j+1}(x) + \frac{1}{\Delta t} u^j(x) \right) u^*(x, \xi) dx = 0, \quad (3)$$

where $\xi \in (a, b)$ is the observation point, $u^*(x, \xi)$ is the fundamental solution. Integrating by parts the first two components of (3) one obtains

$$\int_a^b \frac{\partial^2 u^{j+1}(x)}{\partial x^2} u^*(x, \xi) dx = \left[u^*(x, \xi) \frac{\partial u^{j+1}(x)}{\partial x} - \frac{\partial u^*(x, \xi)}{\partial x} u^{j+1}(x) \right]_a^b + \int_a^b u^{j+1}(x) \frac{\partial^2 u^*(x, \xi)}{\partial x^2} dx$$

and

$$\int_a^b \frac{\partial u^{j+1}(x)}{\partial x} u^*(x, \xi) dx = \left[u^*(x, \xi) u^{j+1}(x) \right]_a^b - \int_a^b u^{j+1}(x) \frac{\partial u^*(x, \xi)}{\partial x} dx$$

so that

$$\begin{aligned} & \int_a^b \left(D \frac{\partial^2 u^{j+1}(x)}{\partial x^2} - c \frac{\partial u^{j+1}(x)}{\partial x} - \frac{1}{\Delta t} u^{j+1}(x) + \frac{1}{\Delta t} u^j(x) \right) u^*(x, \xi) dx \\ &= D \left[u^*(x, \xi) \frac{\partial u^{j+1}(x)}{\partial x} - \frac{\partial u^*(x, \xi)}{\partial x} u^{j+1}(x) \right]_a^b + D \int_a^b u^{j+1}(x) \frac{\partial^2 u^*(x, \xi)}{\partial x^2} dx \\ & - c \left[u^*(x, \xi) u^{j+1}(x) \right]_a^b + c \int_a^b u^{j+1}(x) \frac{\partial u^*(x, \xi)}{\partial x} dx \\ & - \frac{1}{\Delta t} \int_a^b u^*(x, \xi) u^{j+1}(x) dx + \frac{1}{\Delta t} \int_a^b u^*(x, \xi) u^j(x) dx. \end{aligned}$$

This may be simplified as

$$\begin{aligned} & \left[D u^*(x, \xi) \frac{\partial u^{j+1}(x)}{\partial x} - D \frac{\partial u^*(x, \xi)}{\partial x} u^{j+1}(x) - c u^*(x, \xi) u^{j+1}(x) \right]_a^b \\ & + \int_a^b \left(D \frac{\partial^2 u^*}{\partial x^2} + c \frac{\partial u^*}{\partial x} - \frac{1}{\Delta t} u^* \right) u^{j+1}(x) dx + \frac{1}{\Delta t} \int_a^b u^j(x) u^*(x, \xi) dx = 0 \end{aligned}$$

or

$$+ u^*(a, \xi) q^{j+1}(a) - q^*(a, \xi) u^{j+1}(a) + c u^*(a, \xi) u^{j+1}(a) - D u^{j+1}(\xi) + P(\xi) = 0 \quad (4)$$

where

$$\begin{aligned} q^{j+1}(x) &= -D \frac{\partial u^{j+1}(x)}{\partial x} \\ -u^*(b, \xi) q^{j+1}(b) + q^*(b, \xi) u^{j+1}(b) - c u^*(b, \xi) u^{j+1}(b) \end{aligned} \quad (5)$$

And

$$P^j(x, \xi) = \frac{1}{\Delta t} \int_a^b u^j(x) u^*(x, \xi) dx \quad (5)$$

The formula (4) is used to calculate the value of $u(\xi, t)$ at subsequent iterations. This appears in matrix-vector form as

$$\mathbf{G} \mathbf{q} - \mathbf{H} \mathbf{u} - \mathbf{u} + \mathbf{P} = \mathbf{0}, \quad (6)$$

where

$$\mathbf{G} = [u^*(a, \xi) - u^*(b, \xi)], \mathbf{H} = [q^*(a, \xi) - c u^*(a, \xi) - q^*(b, \xi) + c u^*(b, \xi)], \text{ and}$$

$$\mathbf{P} = \frac{1}{\Delta t} \int_a^b u^j(x) u^*(x, \xi) dx.$$

It should be noted that any two of the boundary values $u^{j+1}(a)$, $u^{j+1}(b)$, $q^{j+1}(a)$, or $q^{j+1}(b)$, is known. The value of \mathbf{P} can be evaluated using numerical integration, using (5) and noting that the term $u^j(x)$ is the approximation from the previous iteration.

Construction of the fundamental solution

Gnewuch and Saunter [4] noted that in mathematical textbooks and also in engineering software packages usually only integral equations for the prototype operators such as the Laplace operator, the biharmonic operator, the Lamé operator, the Stokes operator are discussed and realised numerically. They then develop the relevant integral equations for the general second order elliptic boundary value problems with constant coefficients

$$L u := -\text{div}(A \text{ grad } u) + 2hb, \nabla u i + c u,$$

since in the farfield, i.e., as $|x|$ becomes large equations with non constant coefficients or nonlinear equations could be linearized. The definition of fundamental solutions for L involves Macdonald functions K_ν which, for example, are stated in [9]. These functions are modified Bessel functions of the second kind and satisfy the differential equation

$$x^2 u'' + x u' - (x^2 + \nu^2) u = 0,$$

for which they are the solution that remains bounded as x tends to infinity on the real line.

They can be given by the following integral representations

$$\begin{aligned} K_\nu(x) &= \left(\frac{\pi}{2x} \right)^{\frac{1}{2}} \frac{e^{-x}}{\Gamma(\nu \frac{1}{2})} \int_0^\infty e^{-t} t^{\nu - \frac{1}{2}} \left(1 + \frac{t}{2x} \right)^{\nu - \frac{1}{2}} dt \\ &= \frac{1}{2} \left(\frac{x}{2} \right)^\nu \int_0^\infty \exp \left(-t - \frac{x^2}{4t} \right) t^{-\nu - 1} dt \end{aligned}$$

Theorem 1 Let $v = c + hb, b_i = 0$. Then $\kappa_0 : \mathbb{R}^d \rightarrow \mathbb{R}$ defined by

$$\kappa_0(x) = \begin{cases} \frac{1}{2\pi \sqrt{\det A}} e^{\langle b, x \rangle_A} \ln \frac{1}{|x|_A} & \text{for } d = 2 \text{ for } d \geq 2 \\ \frac{1}{(d-2)\omega_d \sqrt{\det A}} \frac{e^{\langle b, x \rangle_A}}{|x|_A^{d-2}} \end{cases}$$

where ω_d is the volume of the unit sphere in \mathbb{R}^d , is a fundamental solution of L . For $v \neq 0$, there exists $\lambda \in \mathbb{C}(-\infty, 0)$ with $\lambda^2 = v$. A fundamental solution κ_λ is given by

$$\kappa_\lambda(x) = \frac{e^{\langle b, x \rangle_A}}{(2\pi)^{d/2} \sqrt{\det A}} \left(\frac{|x|_A}{\lambda} \right)^{1 - \frac{d}{2}} K_{\frac{d}{2}-1}(\lambda |x|_A), \quad x \neq 0$$

The proof of this theorem can still be found in [6]. The symbols hb, x_i and $\|x\|_A$ represent the weighted inner product and weighted norm in \mathbb{R}^d , respectively, and are defined by

$$hb, x_i = \mathbf{b}^T \mathbf{A} \mathbf{x} \text{ and } \|x\|_A = \sqrt{\langle x, x \rangle} = \sqrt{\sum_{i=1}^d a_i x_i^2}$$

Now, for $d = 1$, one obtains

$$\kappa_\lambda(x) = \frac{e^{\langle b, x \rangle_A}}{(2\pi)^{1/2} \sqrt{\det A}} \left(\frac{|x|_A}{\lambda} \right)^{1/2} K_{-1/2}(\lambda \|x\|_A), \quad x \neq 0$$

Taking this to the problem at hand means that a fundamental solution $u^*(x, \xi)$ is

sought which should fulfil the equation

$$\frac{\partial^2 u^*}{\partial x^2}(x, \xi) + \frac{c}{D} \frac{\partial u^*}{\partial x}(x, \xi) - \frac{1}{D\Delta t} u^*(x, \xi) = -\delta(x, \xi)$$

where $\delta(x, \xi)$ is the Dirac delta function with the property

$$\int_{-\infty}^{\infty} \delta(x, \xi) u(x) dx = u(\xi)$$

The fundamental solution $u^*(x, \xi)$ can now be written as

$$u^*(x, \xi) = \left(\frac{|x - \xi|}{2\pi k}\right)^{1/2} e^{-r(x-\xi)} K_{-1/2}(k|x - \xi|), \quad x - \xi \neq 0$$

where $r = c/D$, $k^2 = 1/(D\Delta t) + r^2$, and

$$K_{-1/2}(z) = (2z)^{-1/2} \int_0^{\infty} \exp\left(-t - \frac{z^2}{4t}\right) t^{-1/2} dt.$$

$$I_{\nu}(z) = \sum_{n=0}^{\infty} \frac{1}{k! \Gamma(k + \nu + 1)} \left(\frac{z}{2}\right)^{2k + \nu}$$

$$K_{\nu}(z) = \frac{\pi}{2} \frac{I_{-\nu}(z) - I_{\nu}(z)}{\sin(\nu\pi)},$$

The solutions to the modified Bessel functions of the first and second kind, may be defined in another way by respectively, when ν is not an integer, and I_{ν} and K_{ν} are the two linearly independent solutions to the modified Bessel's equation.

Some selected identities are

$$I_{-\frac{1}{2}}(z) = \sqrt{\frac{2}{\pi z}} \cosh(z) \text{ and } I_{\frac{1}{2}}(z) = \sqrt{\frac{2}{\pi z}} \sinh(z)$$

$$I'_{\nu}(z) = \frac{\nu}{z} I_{\nu}(z) + I_{\nu+1}(z)$$

from which one can write

$$\begin{aligned} K_{-\frac{1}{2}}(z) &= \frac{\pi}{2} \frac{I_{\frac{1}{2}}(z) - I_{-\frac{1}{2}}(z)}{\sin(-\frac{1}{2}\pi)} \\ &= -\frac{\pi}{2} \sqrt{\frac{2}{\pi z}} (\sinh(z) - \cosh(z)); \\ &= \sqrt{\frac{\pi}{2}} z^{-\frac{1}{2}} e^{-z}, \quad z > 0 \end{aligned}$$

Now, the expression for the fundamental solution may be simplified, by substituting for $K_{-1/2}(z)$ as

$$\begin{aligned} u^*(x, \xi) &= \left(\frac{|x - \xi|}{2\pi k}\right)^{1/2} e^{-r(x-\xi)} \sqrt{\frac{\pi}{2}} (k|x - \xi|)^{-\frac{1}{2}} e^{-k|x-\xi|} \\ &= \left(\frac{|x - \xi|}{2k\pi} \cdot \frac{\pi}{2} \cdot \frac{1}{k|x - \xi|}\right)^{1/2} \exp(-r(x - \xi) - k|x - \xi|) \quad (7) \\ &= \frac{1}{2k} \exp(-r(x - \xi) - k|x - \xi|). \end{aligned}$$

It can be verified that

$$\frac{\partial u^*}{\partial x} = \frac{1}{2k} (-r - k \operatorname{sgn}(x - \xi)) \exp(-r(x - \xi) - k|x - \xi|)$$

and

$$P^j(\xi) = \frac{1}{\Delta t} \int_a^b \left(u^j(x) \frac{1}{2k} \exp(-r(x - \xi) - k|x - \xi|)\right) dx.$$

Applying boundary conditions

A numerical scheme is then applied to solve the system (6), by approximating $u(x,t)$ at each time step. At this point, the common practice is that one uses (6), sets the value of the observation points to $\xi = [a,b]$, to determine any two of u_1, u_N, q_1, q_N that may be unknown. Then, (6) is used again to solve for any of the unknown values u_2, \dots, u_{N-1} . In this work, the procedure has been made

easy, especially considering that this has to be done several times basing on the number of time steps. Here, $\mathbf{u} = (u_1, u_2, \dots, u_N)$, $\mathbf{u}^- = (u_1, u_N)$, and $\mathbf{q}^- = (q_1, q_N)$. If all the unknowns, say, q_1, q_N and u_2, \dots, u_{N-1} are brought to the left-hand-side and the knowns u_1, u_N taken to the right-hand-side, then the system (6) appears as

$$\begin{bmatrix} -G_{11} & 0 & \dots & 0 & -G_{12} \\ -G_{21} & 1 & \dots & 0 & -G_{22} \\ \vdots & \vdots & \ddots & \vdots & \vdots \\ -G_{N-1,1} & 0 & \dots & 1 & -G_{N-1,2} \\ -G_{N,1} & 0 & \dots & 0 & -G_{N,2} \end{bmatrix} \begin{bmatrix} q_1 \\ u_2 \\ \vdots \\ u_{N-1} \\ q_N \end{bmatrix} = - \begin{bmatrix} H_{11} + 1 & H_{12} \\ H_{21} & H_{22} \\ \vdots & \vdots \\ H_{N-1,1} & H_{N-1,2} \\ H_{N,1} & H_{N,2} + 1 \end{bmatrix} \begin{bmatrix} u_1 \\ u_N \end{bmatrix} + \mathbf{P}$$

In other words, this takes the form $\mathbf{Ax} = \mathbf{b}$. The complete code that is used to generate all results presented in this work was developed in matlab.

Test problems

The advection–diffusion in 1D has been considered, with different parameters, and initial and boundary conditions. Two test problems are here solved using BEM with time–discretisation and results shown in tables and plotted in graphs. The first problem is a travelling wave while the second takes the form of a wave that diffuses faster than it travels, and both have a known analytical solution. In all cases, the results of the approximations are compared with the exact solution.

Problem 1

Consider the equation

$$\frac{\partial u}{\partial t}(x, t) = D \frac{\partial^2 u}{\partial x^2}(x, t) - c \frac{\partial u}{\partial x}(x, t) \quad (8)$$

with $[a,b] = [-0.75, 1.25]$, $D = 0.01$, $c = 1.0$, and the following initial condition

$$u(x, 0) = \exp\left(-\frac{(x + 0.5)^2}{0.00125}\right).$$

The boundary conditions can be obtained from the known analytical solution to this equation, which is

$$u(x, t) = \frac{0.025}{\sqrt{0.000625 + 0.02t}} \exp\left(-\frac{(x + 0.5 - t)^2}{0.00125 + 0.04t}\right)$$

Figures 1, 2 and 3 show the graphs of the exact and numerical solutions using BEM with time–discretisation for different Δx and Δt . For small step sizes where the nodes are quite many, the plotted values have been limited so as to have clear diagrams. For selected points, $(-0.375, 0.2)$, $(-0.25, 0.3)$, $(-0.125, 0.4)$, $(0.0, 0.5)$, the errors have been computed and tabulated. Table 1 shows errors at these points for $\Delta t = 0.0125$ and Table 2 shows errors for $\Delta t = 0.005$. The step length has been varied as $\Delta x = 0.005, 0.0025, 0.00125$, and 0.0005 in both tables. The figures show that for a given choice of $\Delta x, \Delta t$, the errors look small, while for others the errors look bigger, suggesting the need to make suitable choices of these two values. On the other hand, the tables indicate that as the step length reduces from 0.0025 to 0.0005 , the errors keep reducing. This is illustrated in Figure 4 where the errors are plotted against $1/\Delta x$.

Problem 2

Consider (8) with a different set of parameters and domain, that is, $c = 0.25, D = 0.01, [a,b] = [0,1], t = [0,1]$. The known exact solution to this problem is

$$u(x, t) = \frac{1}{\sqrt{1+t}} \exp\left(-\frac{(x - (1+t)c)^2}{4D(1+t)}\right)$$

The initial and boundary conditions have been obtained directly from the analytical solution. The analytical solution at different times is shown in Figure 5. Computations are made for different choices of $\Delta x, \Delta t$ and results tabulated. Here the different choices of Δx are $0.005, 0.0025, 0.00125$, and 0.0005 , and corresponding to each, Δt has been chosen to be 0.05 and 0.025 . The graphs in Figures 6, 7, 8 show the comparison between the analytical and numerical solutions at selected times $t = 0.3, 0.5, 0.8$, and 1.0 . Again, the number of points plotted has been limited to 20, in order to have clear diagrams. Errors have been computed at selected nodes for different choices of $\Delta x, \Delta t$. Table 3 shows the errors at selected points (x,t) , for $\Delta t = 0.05$ and Table 4 shows the errors at selected points (x,t) , for $\Delta t = 0.025$. For different points (x,t) , the

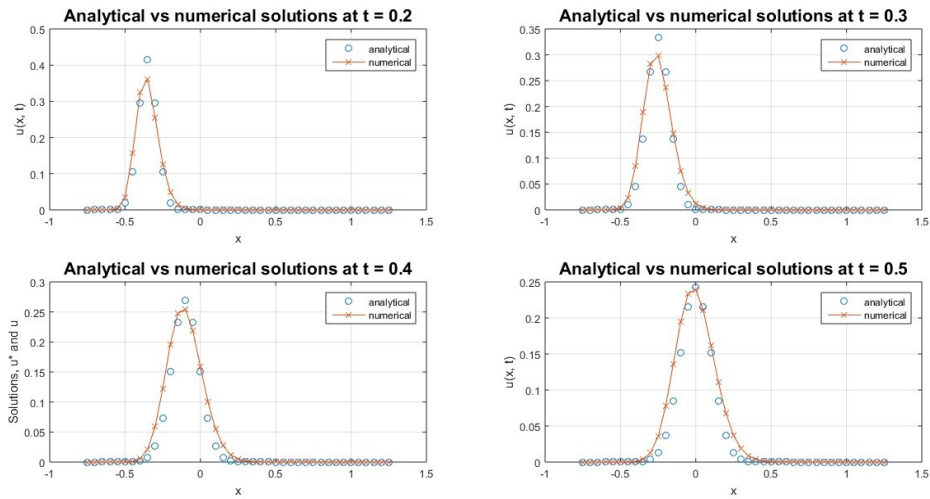


Figure 1. BEM solution to Problem 1 with $\Delta x = 0.0025$, $\Delta t = 0.0125$.

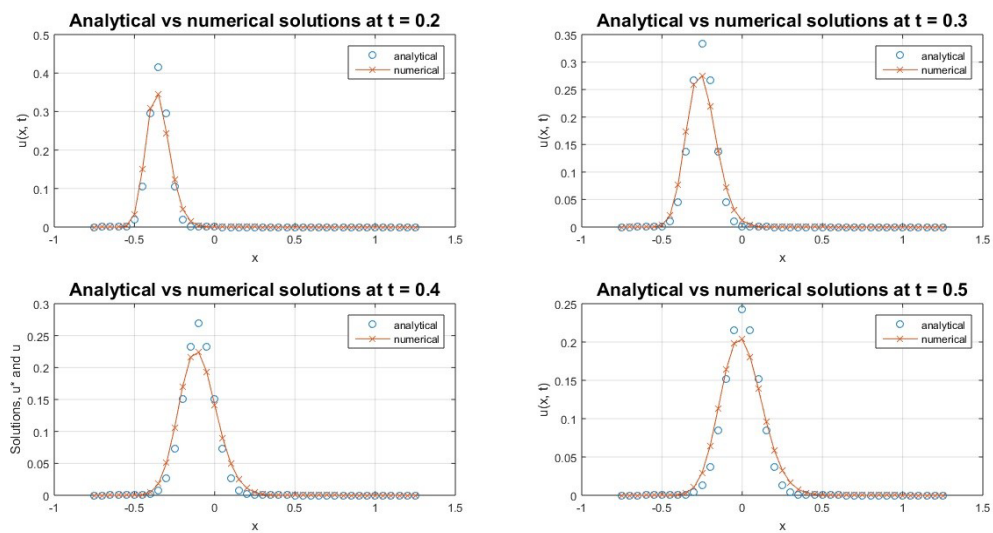


Figure 2. BEM solution to Problem 1 with $\Delta x = 0.00125$, $\Delta t = 0.0125$.

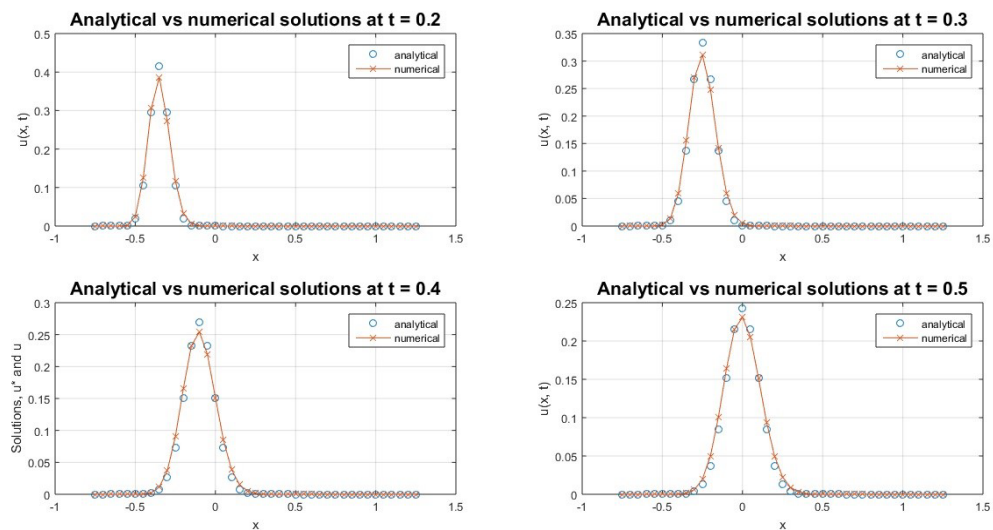


Figure 3. BEM solution to Problem 1 with $\Delta x = 0.0005$, $\Delta t = 0.005$.

Table 1. Errors in BEM solution to Problem 1 for $\Delta x = 0.00125, \Delta t = 0.0125$.

(x,t)	Δx			
	0.005	0.0025	0.00125	0.0005
(-0.375, 0.2)	0.075310588	0.015791865	0.032893340	0.037559268
(-0.25, 0.3)	0.071148136	0.035472962	0.057824564	0.063806427
(-0.125, 0.4)	0.184590869	0.002523138	0.034038790	0.042187089
(0, 0.5)	0.206591963	0.003576774	0.039062113	0.048060057

Table 2. Errors in BEM solution to Problem 1 for $\Delta x = 0.0005, \Delta t = 0.005$.

(x,t)	Δx			
	0.0025	0.00125	0.0005	0.00025
(-0.375, 0.2)	0.171551877	0.024462163	0.009432274	0.014045564
(-0.25, 0.3)	0.262077163	0.025397613	0.022389624	0.028687495
(-0.125, 0.4)	0.462994357	0.056669105	0.009079623	0.017297719
(0, 0.5)	0.614353939	0.065682568	0.011551713	0.020893886

Table 3. Errors in BEM solution to Problem 2 at $\Delta t = 0.05$.

(x,t)	Δx			
	0.005	0.0025	0.00125	0.0005
(0.25, 0.25)	0.019310635	0.001762635	0.002593920	0.003811573
(0.50, 0.25)	0.006243614	0.008666152	0.012374016	0.013410813
(0.25, 0.5)	0.041561936	0.001145649	0.008737007	0.011488490
(0.50, 0.5)	0.014517337	0.021029986	0.029748328	0.032177517
(0.25, 0.75)	0.050546509	0.012212828	0.027337446	0.031532791
(0.50, 0.75)	0.036945324	0.020917836	0.034911137	0.038796103

Table 4. Errors in BEM solution to Problem 2 at $\Delta t = 0.025$.

(x,t)	Δx			
	0.005	0.0025	0.00125	0.0005
(0.25, 0.25)	0.104256469	0.023171716	0.003747977	0.001631469
(0.50, 0.25)	0.091891180	0.017378129	0.000544418	0.005513269
(0.25, 0.5)	0.221045365	0.038481292	0.002884489	0.014180128
(0.50, 0.5)	0.207514469	0.035348301	0.003897015	0.014629829
(0.25, 0.75)	0.324410460	0.035420633	0.026539310	0.043224955
(0.50, 0.75)	0.346911481	0.060621192	0.001147617	0.017807569

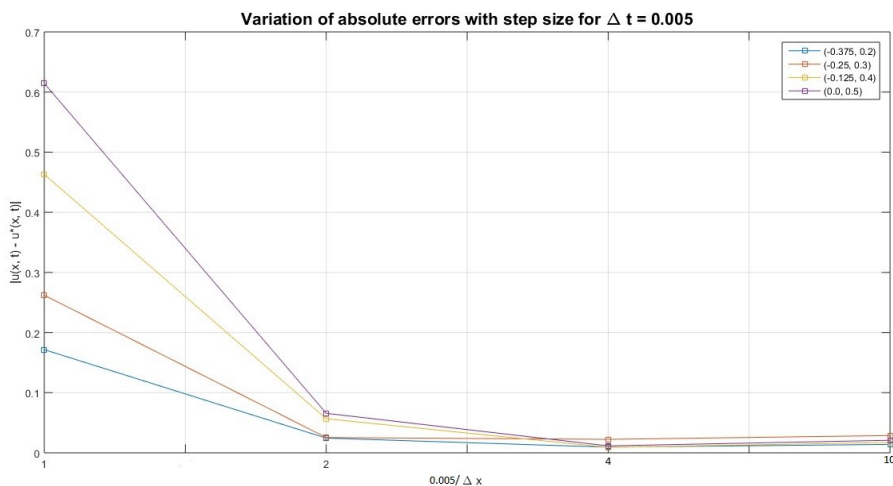


Figure 4. Variation of errors with step length in $u(x,t)$ for Problem 1.

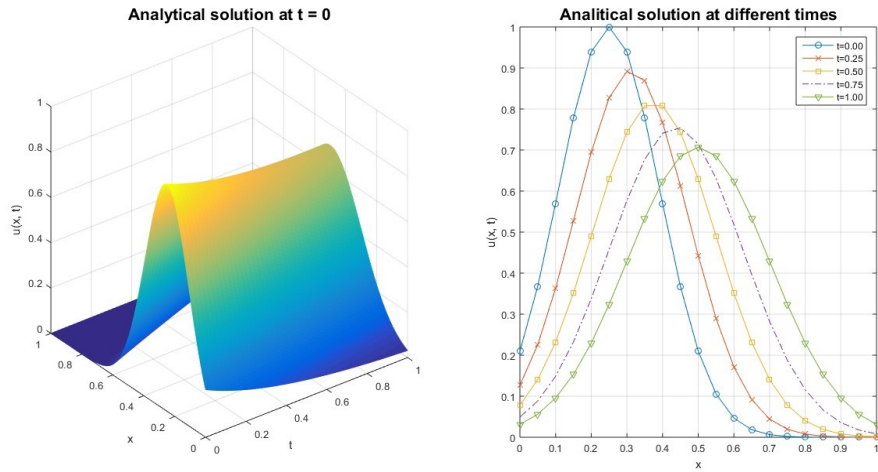


Figure 5. Analytical solution to Problem 2 at different times.

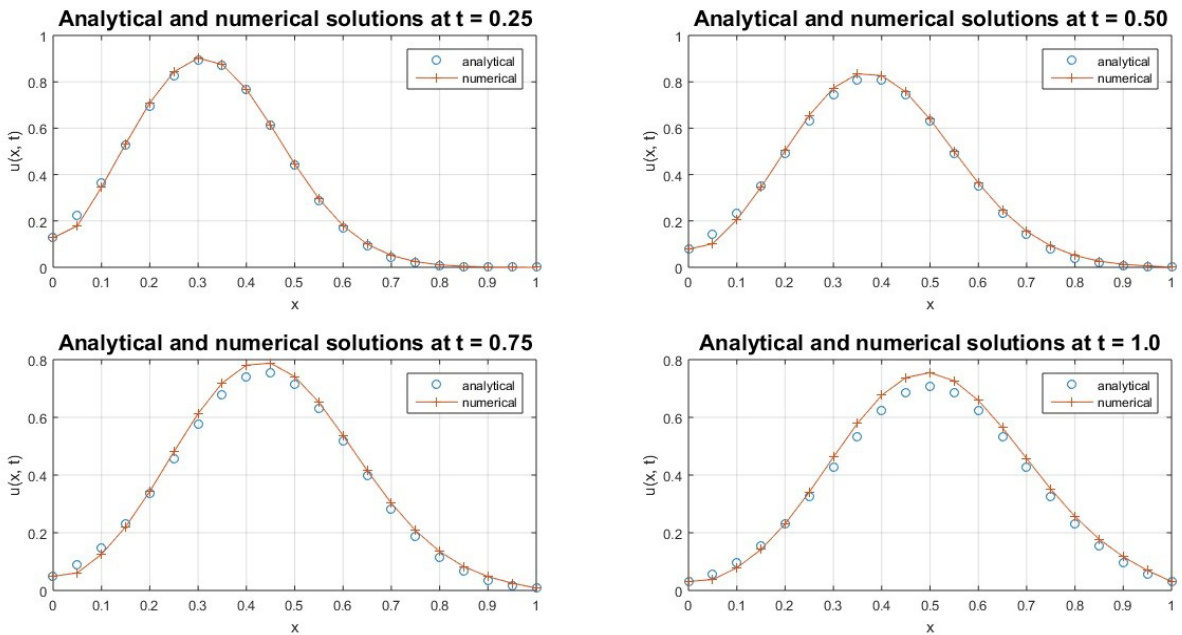


Figure 6. BEM solution to Problem 2 with $\Delta x = 0.005, \Delta t = 0.05$.

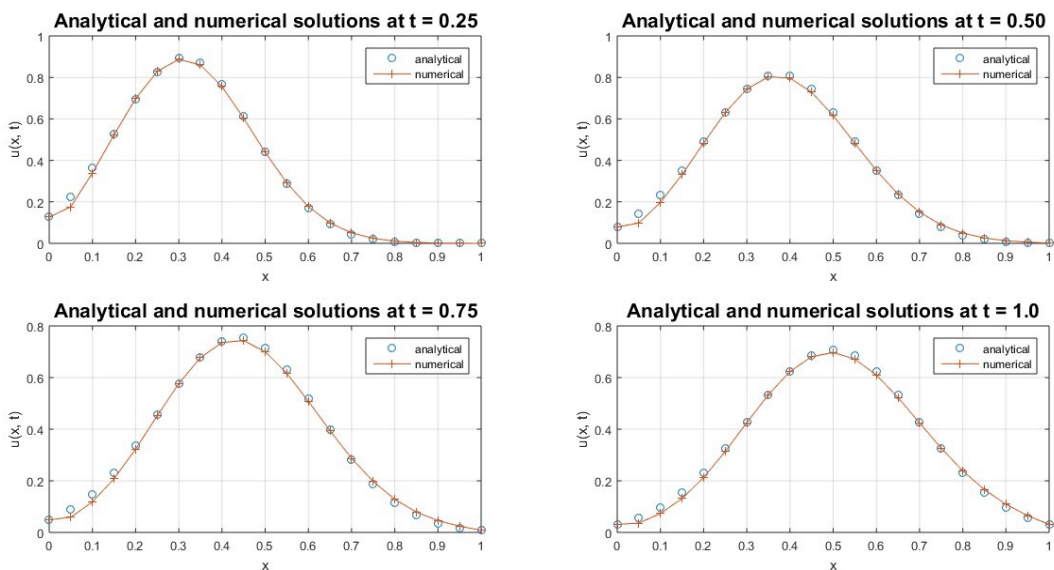


Figure 7. BEM solution to Problem 2 with $\Delta x = 0.0025, \Delta t = 0.05$.

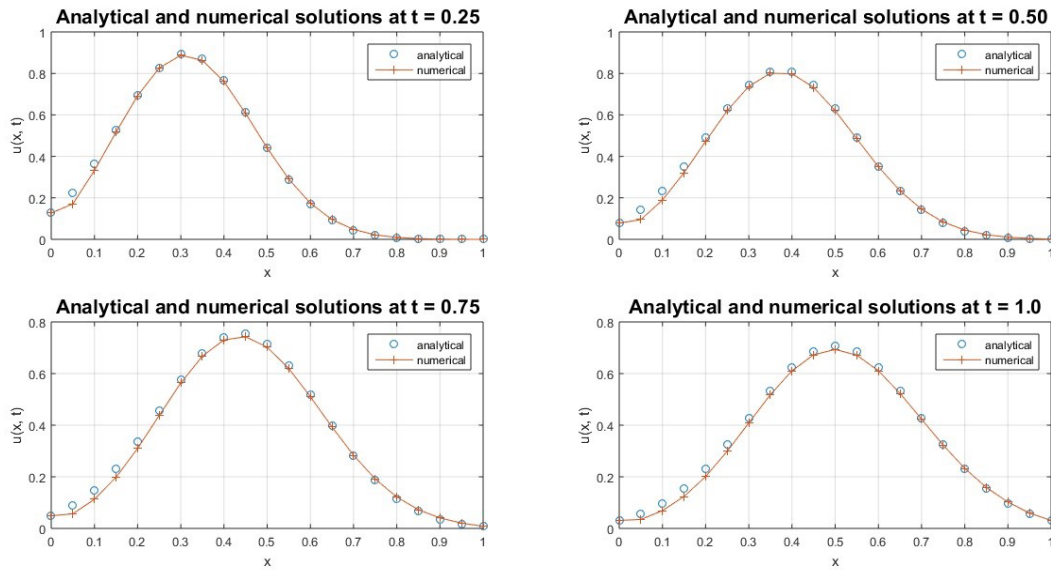


Figure 8. BEM solution to Problem 2 with $\Delta x = 0.0005, \Delta t = 0.025$.

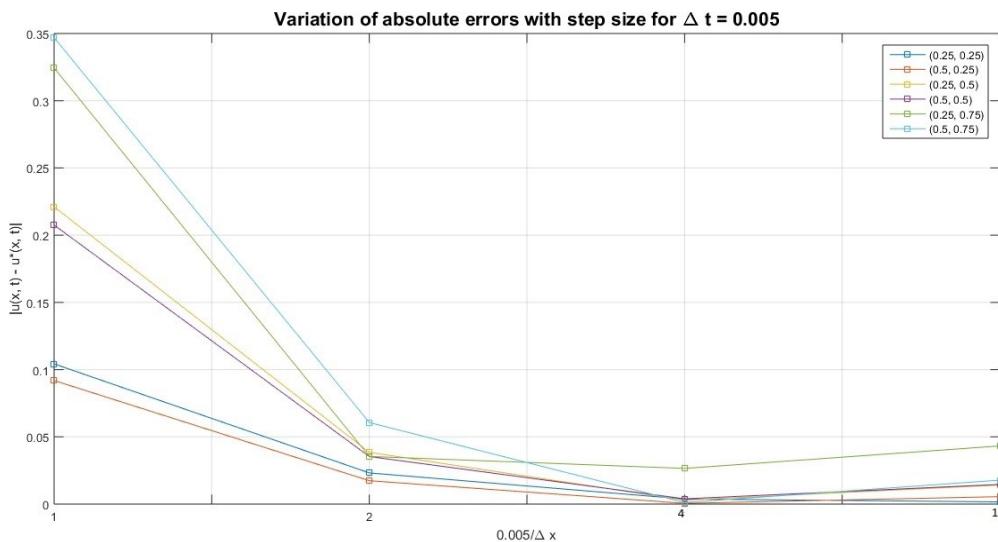


Figure 9. Variation of errors at $x = 0.25$ for Problem 2 with $\Delta t = 0.05$.

variation of the errors at $\Delta t = 0.025$ is shown in Figure 9, indicating that errors reduce with reducing step size.

Discussion of Results

The stability of the suggested method applied to the advection–diffusion equation is here investigated by making various choices of step sizes, in space and time. Two parameters, Peclet number (Pe) and Courant number (Cr), among others, are often used to define

stability and consistency. These are defined as

$$Pe = \frac{c}{D} \Delta x \text{ and } Cr = c \frac{\Delta t}{\Delta x}.$$

The stability of the numerical scheme increases as the Peclet and Courant numbers decrease. The values of Δx that have been used in this work range from 0.25 down to

0.000625, suggesting that for Test Problem 1, say, Pe ranges from 25 down

to 0.0625 since Table 3: Errors in BEM solution to Problem 2 at $\Delta t = 0.05, c = 1.0$ and $D = 0.01$. For these small values of Pe , this will immediately imply that for a fixed time step of $\Delta t = 0.025$ or less, the method is stable. On the other hand, take for example Test Problem 1 with $\Delta x = 0.005, \Delta t = 0.125$ which suggests a very high Courant number, $Cr = 25$ compared with $\Delta x = 0.0125, \Delta t = 0.005$, giving $Cr = 0.4$ and use BEM to find the approximation. These results are illustrated in Figure 10, showing the difference in approximations for both a high and low Cr , in terms of shapes of the graphs. Convergence means that the solution to the finite difference approximation approaches the true solution of the PDE when the mesh is refined. As a test for convergence it is required to determine whether the solutions with increasingly refined domains approach a fixed value. Additionally, since the analytical solution is known, one tests whether this sequence of solutions converges to this value, and this is known as consistency. BEM was applied to the Test Problem 1 using the time steps, $\Delta t = 0.25, 0.125, 0.05, 0.005$ for different step lengths, $\Delta x = 0.0025, 0.00125, 0.0005$. From the results, a value of $\Delta t = 0.005$ was determined to be sufficiently small to give convergence. Figures 11 & 12 shows the results obtained at $t = 0.5$ for reducing step lengths, up to $\Delta x = 0.0025$. The convergence of BEM is attained when the choice $\Delta x = 0.0005, \Delta t = 0.005$ is

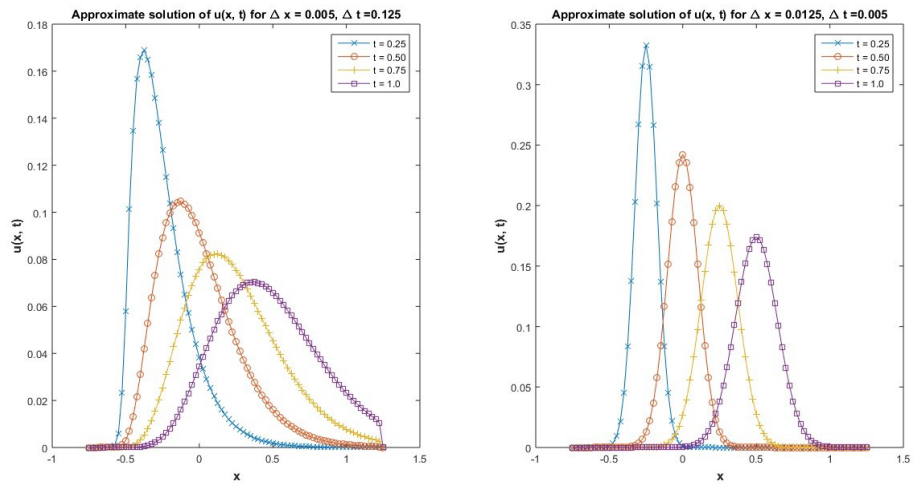


Figure 10. BEM solution to Problem 1 at different times when (a) $Cr = 25$ and (b) $Cr = 0.4$.

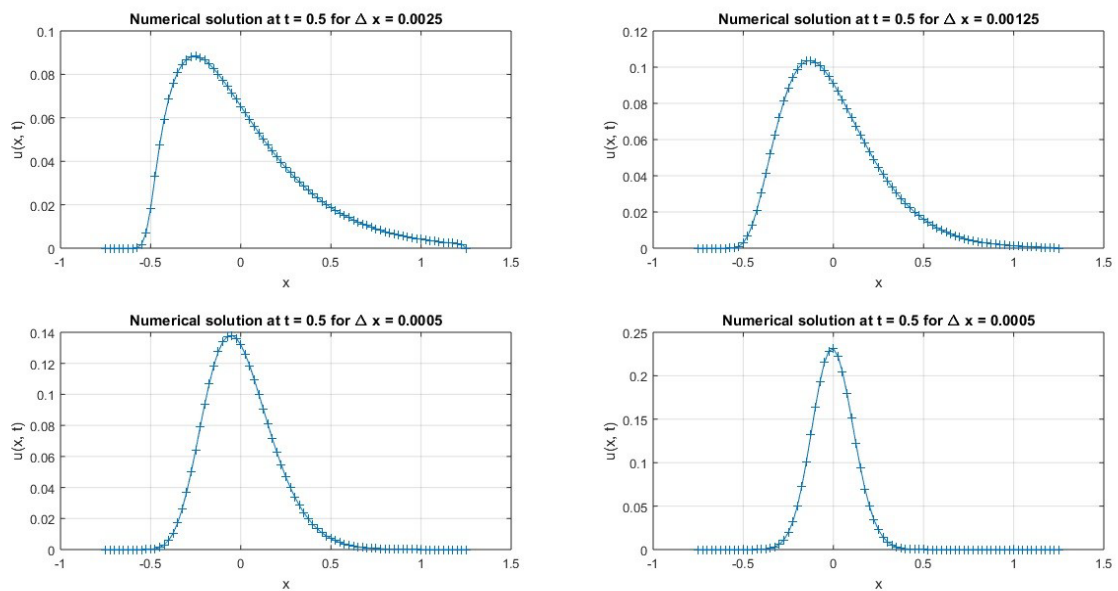


Figure 11. BEM solution to Problem 1 at $t = 0.5$ with different Δx .

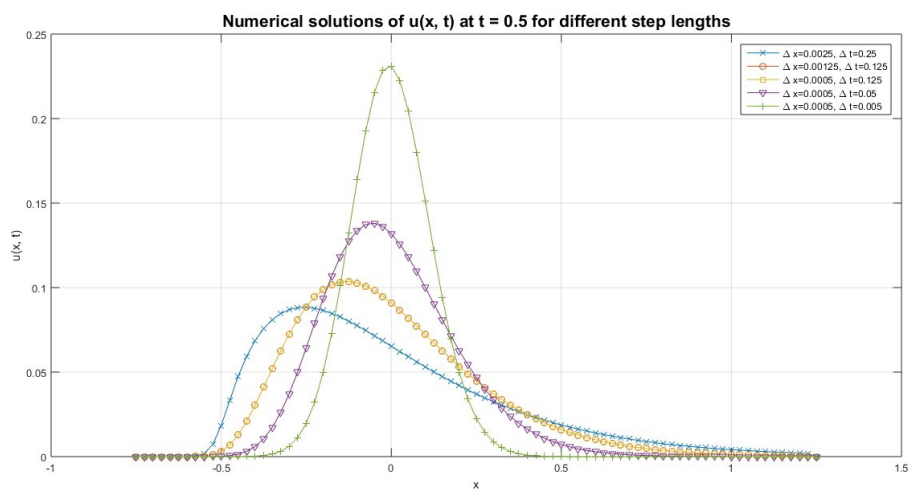


Figure 12. Comparison of BEM solution to Problem 1 at $t = 0.5$ with different Δx .

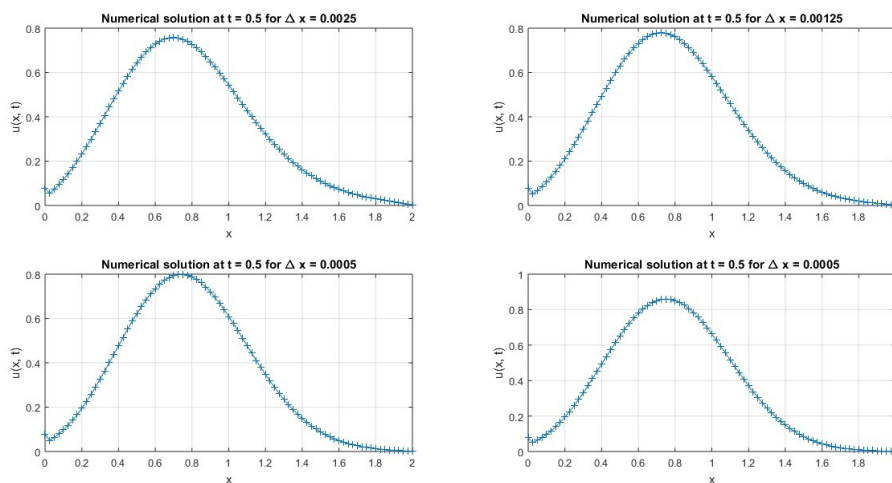


Figure 13. BEM solution to Problem 2 at $t = 0.5$ with different Δx .

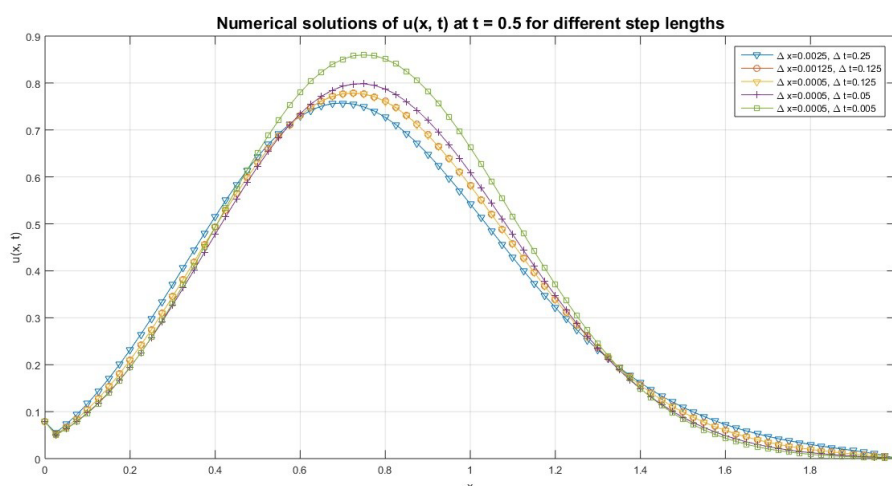


Figure 14. Comparison of BEM solution to Problem 2 at $t = 0.5$ with different Δx .

Table 5. Errors in BEM solution to Problem 1 at $t = 0.5$.

$(x, 0.5)$	Δx						Exact
	0.025	0.0125	0.00625	0.0025	0.00125	0.000625	
0.2500	0.0903	0.0936	0.0770	0.0452	0.0294	0.0203	0.0128
0.3125	0.0828	0.1078	0.1298	0.1418	0.1394	0.1366	0.1163
0.3750	0.0660	0.0937	0.1268	0.1731	0.2035	0.2382	0.2425
0.4375	0.0511	0.0691	0.0883	0.1087	0.1174	0.1255	0.1163
0.5000	0.0372	0.0457	0.0489	0.0420	0.0325	0.0232	0.0128
0.5625	0.0269	0.0281	0.0230	0.0113	0.0050	0.0017	0.0003
0.6250	0.0188	0.0163	0.0095	0.0023	0.0005	0.0001	0.0000

made, and subsequent reductions in both step sizes shall lead to little change in the approximation results. Table 5 gives results for reducing step lengths, showing that the first columns contain quite different values from the rest, but continuously improving as the step length reduces, and in the end the values are within the same range, indicating that a point of convergence has been attained. Now, Test Problem 2 is solved using BEM with time steps, $\Delta t = 0.25, 0.125, 0.05$ for different step lengths, $\Delta x = 0.0025, 0.00125, 0.0005$. From the results, a value of $\Delta t = 0.05$ was determined to be sufficiently small to give convergence. Starting with a maximum of $\Delta x = 0.0025$, convergence was determined by successively reducing the step length up to $\Delta x = 0.0005$. Figure 13 shows the results obtained at $t = 0.5$ for reducing step lengths. These graphs appear to have a similar shape, though they do not fit into each other,

as shown in Figure 14. The values indicate that BEM is convergent when the choice $\Delta x = 0.0005, \Delta t = 0.05$ is made, because subsequent reductions in both step sizes lead to little change in the approximation results. The graphs are initially distinguished, though they tend to one point as the step length reduces, indicating that a point of convergence has been attained.

Conclusion

The errors in approximations have been studied, noting that for this method, errors in the approximations reduce with decreasing grid size. The stability, convergence, and consistency of BEM applied to the advection–diffusion equation have been discussed. The stability of the method was tested using

the concept the Peclet and Courant numbers. Basing on the Table 5: Errors in BEM solution to Problem 1 at $t = 0.5$. results from the simulations, it was found that the method considered was stable. Again, for this method, several solutions with different values of distance and time steps have been obtained to ensure that the solution does not depend on the model discretisation. This has been done by repeatedly generating simulations with reduced distance and time steps and analysing the output at selected times over the domain. It was found that the method is convergent since further refinement of distance and time steps produced insignificant change in the model output. The results were presented in a number of tables and illustrated using graphs, all generated using MATLAB.

References

1. Goong C and Jianxin Z. "Boundary element methods with applications to nonlinear problems." *Springer Science & Business Media* 7(2010).
2. Alexander C and Daisy T. "Heritage and early history of the boundary element method." *Engineering Analysis with Boundary Elements* 29(2005):268-302.
3. Majchrzak E, Ewa L, Jerzy M and Alicja PB. "Different variants of the boundary element method for parabolic equations." *Scientific Research of the Institute of Mathematics and Computer Science* 3(2004):127-132.
4. Maria L and Ewa L. "Application of the boundary element method using discretization in time for numerical solution of hyperbolic equation." *Scientific Research of the Institute of Mathematics and Computer Science* 7(2008):83-92.
5. Ewa, Majchrzak. "Solution of dual phase lag equation by means of the boundary element method using discretization in time." *JACM* 12(2013):89-95.
6. Michael G, Stefan A Sauter. *Boundary integral equations for second order elliptic boundary value problems.* (1999).
7. Mehdi D, Jalil M and Abbas S. "The solution of the linear fractional partial differential equations using the homotopy analysis method." *Zeitschrift für Naturforschung-A* 65(2010):935.
8. Tanaka M, Matsumoto T and Takakuwa S. "Dual reciprocity bem based on time-stepping scheme for the solution of transient heat conduction problems." *WIT Transactions on Modelling and Simulation*, 35 (2003).
9. Grant M. "Symmetric functions and Hall polynomials." *Oxford university press* 1998.

How to cite this article: Ronald Mwesigwa, Godwin Kakuba and David Angwenyi. The Fundamental Solution of the One-Dimensional Elliptic Operator and its Application to Solving the Advection-Diffusion Equation. *J Appl Computat Math* 9 (2020) doi: 10.37421/jacm.2020.9.458